Published in final edited form as:
J Biol Inorg Chem. 2013 March ; 18(3): 371–381. doi:10.1007/s00775-013-0981-9.

Ferritin and ferrihydrite nanoparticles as iron sources for *Pseudomonas aeruginosa*

Carolyn Dehner,
Department of Chemistry and Biochemistry, University of Notre Dame, Notre Dame, IN 46556, USA

Nydia Morales-Soto,
Department of Civil and Environmental Engineering, and Earth Sciences, University of Notre Dame, Notre Dame, IN 46556, USA

Department of Biological Sciences, University of Notre Dame, Notre Dame, IN 46556, USA

Rabindra K. Behera,
Children's Hospital Oakland Research Institute, Oakland 94609, USA

Joshua Shrout,
Department of Civil and Environmental Engineering, and Earth Sciences, University of Notre Dame, Notre Dame, IN 46556, USA

Department of Biological Sciences, University of Notre Dame, Notre Dame, IN 46556, USA

Elizabeth C. Theil,
Children's Hospital Oakland Research Institute, Oakland 94609, USA

Patricia A. Maurice, and
Department of Civil and Environmental Engineering, and Earth Sciences, University of Notre Dame, Notre Dame, IN 46556, USA

Jennifer L. Dubois
Biosciences Division, Center for Infectious Diseases, and Biodefense Research, SRI International, 140 Research Drive, Harrisonburg, VA 22802, USA jennifer.dubois@sri.com

Abstract

Metabolism of iron derived from insoluble and/ or scarce sources is essential for pathogenic and environmental microbes. The ability of *Pseudomonas aeruginosa* to acquire iron from exogenous ferritin was assessed; ferritin is an iron-concentrating and antioxidant protein complex composed of a catalytic protein and caged ferrihydrite nanomineral synthesized from Fe(II) and O_2 or H_2O_2. Ferritin and free ferrihydrite supported growth of *P. aeruginosa* with indistinguishable kinetics and final culture densities. The *P. aeruginosa* PAO1 mutant (Δ*pvdD*Δ*pchEF*), which is incapable of siderophore production, grew as well as the wild type when ferritin was the iron source. Such data suggest that *P. aeruginosa* can acquire iron by siderophore-independent mechanisms, including secretion of small-molecule reductant(s). Protease inhibitors abolished the growth of the siderophore-free strain on ferritins, with only a small effect on growth of the wild type; predictably, protease inhibitors had no effect on growth with free ferrihydrite as the iron source. Proteolytic activity was higher with the siderophore-free strain, suggesting that the role of

Correspondence to: Jennifer L. Dubois.

Present Address:, C. Dehner, Biochemistry Program, Smith College, Northampton, MA, USA
Present Address: R. K. Behera, Department of Chemistry and Biochemistry, University of South Carolina, Columbia, SC, USA

proteases in the degradation of ferritin is particularly important for iron acquisition in the absence of siderophores. The combined results demonstrate the importance of both free ferrihydrite, a natural environmental form of iron and a model for an insoluble form of partly denatured ferritin called hemosiderin, and caged ferritin iron minerals as bacterial iron sources. Ferritin is also revealed as a growth promoter of opportunistic, pathogenic bacteria such a *P. aeruginosa* in diseased tissues such as the cystic fibrotic lung, where ferritin concentrations are abnormally high.

Keywords

Iron acquisition; Ferritin; Ferrihydrite; Siderophore; *Pseudomonas aeruginosa*

Introduction

Iron is essential for nearly all microbes but is poorly accessible and therefore growth-limiting in many environments. In the extracellular fluids of the human body, iron is tightly sequestered in heme-containing proteins and transporters such as transferrin and lactoferrin. The importance of acquisition of iron from these sources to pathogen survival is well established [1–6]. In contrast to transferrin and heme, the iron storage protein ferritin has received little attention as a potential microbial iron source. Ferritin protein cages synthesize internal nanominerals from Fe(II) and O_2 or H_2O_2 with a ferrihydrite structure. Whereas only approximately 0.1 % of iron in humans circulates in the plasma protein transferrin, nearly 25 % is concentrated inside cytoplasmic ferritin; each ferritin nanomineral contains up to 4,000 iron atoms, making it a potentially rich iron source for pathogens. However, because of the low solubility of ferrihydrite, the primarily intracellular location of ferritin, and the apparent lack of direct receptor-mediated mechanisms for ferritin uptake by most bacteria [7], iron from ferritin has been assumed to be unavailable to extracellular pathogens. Moreover, under normal conditions, ferritin is present in low concentrations in the extracellular milieu. Plasma concentrations of ferritin are only 1.5–30 ng/ ml, compared with 200–320 μg/ml for transferrin [8, 9].

Extracellular ferritin concentrations in other body fluids such as sputum and bronchoalveolar lavage (BAL) fluid range from similar to modestly higher compared with those in serum in normal, healthy individuals (about 200 ng/ml in sputum and about 9 ng/ml in BAL fluid) [10, 11]. However, just as in serum, extracellular concentrations of ferritin in these lung fluids increase in disease states, in some cases dramatically. For example, in one study an approximately 70-fold increase in extracellular ferritin concentration in BAL fluid from the lungs of cystic fibrosis (CF) patients, compared with healthy controls, was reported [11]; other studies have shown an approximately 20-fold increase extracellular ferritin concentration in sputum [10, 12–14]. This suggests that ferritin iron could be an important iron source for opportunistic pathogens of CF patients, exemplified by clinically important strains of *Pseudomonas aeruginosa*. Whether extracellular ferritin is enriched in diseases other than CF (measured in sputum) or in cases of iron overload/inflammation (measured in serum) is not yet known. In addition, abiotic ferrihydrites and ferritins in some plant seeds and bacteria are present in a wide variety of natural environments [15–18]. Since the potential availability of ferritin iron and ferrihydrite iron has both biomedical and environmental implications, we investigated whether and by what mechanism(s) ferrihydrite iron and ferritin iron can be used as iron sources by the well-described environmental and clinical pathogen *P.aeruginosa*.

P. aeruginosa strains have several mechanisms that could contribute to acquisition of iron from ferritin or ferrihydrite. In one mechanism, based on chelation, two high-affinity siderophores are synthesized and secreted to competitively bind and move Fe(III) through

the outer membrane via TonB-mediated transport [4]. Siderophores also enhance ferrihydrite dissolution rates to facilitate metabolism of iron (hydr)oxide minerals. In a second mechanism, low-affinity iron chelators and exogenous reductants such as pyocyanin are synthesized and secreted [19]. Pyocyanin can mediate acquisition of iron from transferrin by reduction of Fe(III) to Fe(II), facilitating transport of hexaquoiron(II) through outer-membrane porins [20]. If ferritin minerals are an iron source for bacteria, bacterial proteases may also play a role in iron acquisition. Some strains of P. aeruginosa isolated from cystic fibrotic lungs, an essentially aerobic environment where free iron exists predominantly as Fe(III), survive without sidero-phores, [21, 22], suggesting another, possibly ferritin-dependent mechanism of iron acquisition in such strains.

The caged ferritin ferrihydrite is nanoparticulate iron oxyhydroxide: approximately 20 % FeO_4 and 80 % FeO_6 polyhedra in addition to water and water-derived hydroxides [15, 17, 23]. Eukaryotic ferritins consist of 24 protein subunits assembled into the protein cage, have a molecular mass of approximately 450 kDa and an interior cavity 7 nm in diameter, and synthesize the caged iron minerals through combining protein-based catalysis and, in eukaryotes, protein-based mineral nucleation; mineral growth occurs in the nanocavity [23, 24]. The two structural forms of free ferrihydrite often studied are the smaller, less-ordered two-line (2L) ferrihydrite and the larger, more-ordered six-line (6L) ferrihydrite, where the number of lines refers to the number of X-ray diffraction maxima [25, 26]. When the iron content per ferritin protein cage is lower, the ferritin mineral resembles 2L ferrihydrite; as the iron content per cage increases, the mineral resembles 6L ferrihydrite [27, 28]. We compared free 2L and 6L ferrihydrite with 2L and 6L ferrihydrite inside ferritin cages for three reasons: (1) structurally distinct, microscale to macroscale iron (oxyhydr)oxide minerals have in the past influenced bacterial iron bioavailability [17, 29–31] and dissolution rates in the presence of siderophores [32]; (2) aggregation of free ferrihydrite [15–17] is faster with 2L ferrihydrite than with 6L ferrihydrite (unpublished observations); (3) ferritin protein cages, which control both mineral synthesis and dissolution [23, 24, 33], may be degraded in diseased tissue [34, 35], exposing the ferrihydrite core (hemosiderin). We compared effects of ferritin and free ferrihydrite on growth, and expression of selected genes, in wild-type and high-affinity siderophore-free, mutant strains.

Materials and methods

Bacterial strains and growth conditions

The strains and plasmids used in this study are listed in Table 1. *P. aeruginosa* strains, all derivatives of *P. aeruginosa* PAO1, were cultivated in lysogeny broth to an absorbance at 600 nm (A_{600}) of 0.8 (mid-logarithmic growth). Cells were collected by centrifugation, resuspended in sterile iron-deficient medium (FeDM), and introduced 1:100 into 50-ml acid-washed flasks containing 20 ml of FeDM as described previously [36]. Chemostats were not used because of the potential for trace iron contamination. For iron-depleted conditions, the medium was used as prepared, with the trace iron present supporting minimal culture growth.

For cultures grown with ferrihydrite or ferritin, the added iron source is expressed in terms of total iron content (5 or 50 μM Fe as indicated). Cultures were incubated at 37 °C at 100 rpm for 48 h. Three hundred microliters of each culture was removed every 6 h to measure the absorbance (A_{600}) and promoter activity (see later); an additional aliquot was removed at 24 h for other assays as needed. Controls containing either ferrihydrite or ferritin, but lacking cells, were also measured to perform normalization for interference with absorbance readings and to determine whether particle dissolution was occurring in the absence of bacteria. For the latter, a microcentrifuge tube filter with a membrane of 10-kDa pore size was used to remove the ferritin/ferrihydrite from the growth medium. The flow-through was

acidified in 2 % HNO3 and analyzed by inductively coupled plasma optical emission spectroscopy (ICP-OES) (see later). All cultures were grown in triplicate in the dark to prevent photocatalyzed reductive dissolution, and the results were averaged. The pH of the culture medium at the end of experiments had typically risen from an initial value of 7.2 to approximately 8.3.

To determine the dependence on proteases for acquisition of iron from ferritin, a water-soluble protease inhibitor cocktail (PIC) from Sigma was added to provide 0.2 mM 4-(2-aminoethyl)benzenesulfonyl fluoride, 0.03 μM aprotinin, 13 μM bestatin HCl, 1.4 μM E64, 100 μM EDTA, and 0.1 μM leupeptin. The PIC is intended to inhibit proteases of different types, but its specific inhibitory properties against particular proteases have not been measured. To evaluate the effect of the EDTA present in the PIC on ferrihydrite dissolution, bioavailability, and acquisition of iron from ferritin, EDTA alone was added instead of the PIC, at a final concentration of 100 μM. Protease detection assays were performed by supplementing 100 ml of FeDM (0.6 % Noble agar) with 8 ml of sterile nonfat dry milk (1 g/10 ml Nanopure H_2O). Protease assay medium was spotted with *P. aeruginosa* PAO1 wild-type and siderophore-free cultures collected at 18 h of growth on 5 μM iron (from 1,500Fe ferritin, where 1,500 refers to the approximate number of iron atoms per protein cage), and diluted to A_{600} of 0.8.

Ferrihydrite and ferritin biomineral synthesis

Samples of 2L and 6L ferrihydrite were synthesized according to methods described by Schwertmann and Cornell [37]. The 6L ferrihydrite was prepared by rapid hydrolysis of an acidic $Fe(NO_3)_3 \cdot 9\ H_2O$ solution through brief heating to 75 °C and subsequent cooling, followed by extensive dialysis. The 2L ferrihydrite was prepared by precipitation through rapid addition of base to reach a neutral pH, followed by several washes with double-distilled H_2O. For samples that were freeze-dried, X-ray diffraction (using Cu Kα radiation) confirmed the samples as 2L or 6L ferrihydrite. Brunauer–Emmett–Teller adsorption isotherm analysis (B20 Micromeritics ASAP 2020 accelerated surface area and porosimetry system) yielded a specific surface area of 284.9 m^2/g for 2L ferrihydrite and 222.8 m^2/g for 6L ferrihydrite.

Ferrihydrite aggregates over time in neutral aqueous solution, decreasing the overall surface area and possibly the reactivity of the nanoparticles [29]. We visually observed that previously freeze-dried ferrihydrite maintained in solution at neutral pH and room temperature formed particle aggregates over the course of several days. Occasionally, mineral aggregates forming from freeze-dried ferrihydrite settled to the bottom of the growth flasks. In these experiments, cultures of wild-type *P. aeruginosa* grew dramatically less (data not shown) on the aggregated ferrihydrite. Ferrihydrite was therefore prepared fresh for use within 3 days in these experiments, and extensive aggregation was not observed.

Recombinant frog M-ferritin was expressed in *Escherichia coli*, purified as described previously [24], and stored in a buffer of 0.1 M 3-(*N*-morpholino)propanesulfonic acid, 0.1 M NaCl, pH 7.0. Ferritin mineralization was achieved by the addition of freshly prepared solutions of $FeSO_4$ (in dilute HCl) in the same buffer. To make ferritin containing a mineral equivalent to either 2L or 6L ferrihydrite, a stock solution of $FeSO_4$ was added to a final molar ratio of 500Fe ferritin (low-iron-loaded ferritin) and 1,500Fe ferritin (high-iron-loaded ferritin). Immediately before use, the protein samples were fractionated on a gel filtration column (Sephacryl-S200, GE Healthcare) to remove any denatured protein or iron not associated with the ferritin, and were then analyzed by native polyacrylamide gel electrophoresis. The iron content of the ferritin used was confirmed by measuring the protein (Bradford assay) and iron (ICP-OES; see later) concentrations after gel filtration.

Transmission electron microscopy

Ferritin samples were diluted in growth medium and airdried on copper grids. These were either left unstained (to image the mineral core) or stained with uranyl acetate (to image the protein cage). Images were collected with a Titan 80–300 with an accelerating voltage of 80 kV. Ferrihydrite samples were prepared in a similar fashion.

Measurement of iron via ICP-OES

Samples were diluted in 2 % HNO_3. Iron concentrations were measured with a PerkinElmer spectrophotometer equipped with an autosampler. Standard curves (more than 10 μg/l) were generated using single element iron standards (CPI International).

β-Galactosidase assay

Promoter-lacZ fusions were constructed in *P. aeruginosa* PAO1 wild-type and siderophore-free strains as described previously [29, 38]. The P_{pvdA} promoter regulates downstream production of messenger RNA in proportion to sensed iron levels, via the iron-binding ferric uptake regulator (Fur) protein [4]. The measured amount of β-galactosidase activity correlates with the degree of iron deprivation, as expected for a Fur-regulated gene. β-Galactosidase expressed under P_{pvdA} control was quantified by the assay previously described by Miller and Hersh-berger [39]. Briefly, 100-μl aliquots of cells (or a dilution thereof) were added to 1 ml of Z buffer (60 mM Na_2H-$PO_4{\cdot}7H_2O$, 40 mM $NaH_2PO_4{\cdot}H_2O$, 10 mM KCl, 1 mM $MgSO4{\cdot}7H_2O$, 50 mM β-mercaptoethanol), 20 μl of fresh 0.1 % sodium dodecyl sulfate, and 40 μl of chloroform. After the chloroform had settled, 100-μl samples of per-meabilized cells were removed into 20 μl of o-nitrophenyl-β-D-galactopyranoside (4 mg/ml) and incubated at room temperature for 20 min before the reaction was quenched with 50 μl of 1 M Na_2CO_3. The absorbance at 420 nm (A_{420}) was measured with a Varian Cary 50 spectrophotometer, and Miller units were determined as 1,000 × (A420)/(TVA_{600}), where T is the reaction time in minutes and V is volume of culture used in the assay in milliliters.

Ferrozine assay for Fe(II)

Reduction of Fe(III) to Fe(II) was measured on the basis of the method of Stookey [40]. Briefly, cultures were grown with ferritin, ferrihydrite, or without added iron for 24 h and 1-ml aliquots were used for the assay. For supernatant samples, cells were gently sedimented and the supernatant was filter-sterilized with a 0.2-um filter. Ferrozine (0.5 mM) and ferric nitrilotriacetic acid (0.2 mM) were added to whole-cell or supernatant samples and the mixtures were incubated at 30 °C with mild shaking (75 rpm). Cofactors were excluded to determine if iron reduction could occur without their addition in the supernatant or at the cell surface. The characteristic absorbance of the Fe(II)–ferrozine complex (A_{562}) was monitored after 30 min, and the value from a medium control (containing the appropriate iron source) was subtracted as the background. The concentration of Fe(II)–ferrozine was calculated using ε = 27.9 mM/cm and referenced per cell (1.8×10^9 cells was equivalent to an absorbance reading of 1.0 at 600 nm).

Pyocyanin assay

Aliquots were removed from cultures at late-log phase, cells were sedimented, and the supernatant was filtered-sterilized. Pyocyanin was then quantified on the basis of the method of Essar et al. [41]. Briefly, 500 μl of this supernatant was extracted with 300 μl of chloroform, and was then re-extracted into 100 μl of 0.2 N HCl to give a pink color typical of pyocyanin in acidic solution. This was diluted 1:2 with double-distilled H_2O, and the absorbance was read at 520 nm. Pyocyanin concentration was calculated and reported in micrograms per milliliter [35, 42].

Results

Characterization of ferritin prior to growth experiments

Unstained transmission electron microscopy (TEM) images clearly show the different sizes of the ferrihydrite mineral core for 500Fe ferritin (Fig. 1a) versus 1,500Fe ferritin (Fig. 1b) samples. Images of samples stained with uranyl acetate reveal the protein cage surrounding the core (Fig. 1c). The ferrihydrite samples proved unsuitable for detailed characterization by TEM owing to extensive aggregation that occurred upon drying.

To ensure that acquisition or iron from these sources was not due to dissolution of the nanominerals by the medium alone, the ferritin and ferrihydrite samples were incubated in growth medium without added bacteria for the duration of a typical experiment. In all samples tested, iron concentrations were below the ICP-OES detection limit (below 10 μg/l).

Availability of iron from ferrihydrites and ferritins to wild-type *P. aeruginosa*

The siderophore-producing wild-type strain of *P. aeruginosa* exhibited robust and identical growth on 2L and 6L ferrihydrite (50 μM Fe), entering log phase quickly and reaching a maximum (A_{600} = 2.2) by 18 h (Fig. 2a). At tenfold lower equivalent iron concentrations (5 μM Fe), growth was delayed and the maxima were less, but growth trends were similar on the two forms of ferrihydrite.

Similar results were observed for growth on ferritin (Fig. 2b). When provided with 1,500Fe ferritin or 500Fe ferritin equivalent to 50 μM iron, the cultures quickly entered log phase, and a culture maximum (A_{600} = 2.0) was observed by 18 h. When the cultures were provided with these ferritins at 5 μM iron, the growth patterns were again nearly identical to each other. Given the similarity between growth on ferritin and ferrihydrite, the ferritin protein coat does not appear to restrict acquisition of iron from the ferrihydrite-core iron by wild-type *P. aeruginosa*.

Availability of iron from ferrihydrites and ferritins to the siderophore-free mutant

The siderophore-free mutant was able to acquire iron from ferrihydrites (50 μM Fe), although with a lag before entering log phase and a lower maximum culture density (A_{600} = 1.7) compared with the wild-type strain (Fig. 3a). When tenfold less ferrihydrite was added (5 μM Fe), growth was more noticeably slowed. The 2L and 6L ferrihydrites were equally available iron sources for this strain.

The siderophore-free strain exhibited the same growth kinetics as the wild-type strain when ferritin was provided at equivalent iron concentrations of either 50 or 5 μM (Fig. 3b). In contrast to the experimental results for the wild type, growth kinetics suggested that iron was more readily acquired by the mutant from ferritins than from ferrihydrites. A biosensor assay was used to assess the cellular iron status via the promoter activity of *pvdA*, which is strongly upregulated under iron starvation [4, 29, 38]. The results of this assay (Fig. 3b) confirm that iron is more readily accessed from ferritin than from ferrihydrite. Promoter activity is lowest in the cultures with 50 μM iron from ferritin (Fig. 3d), and highest with 5 μM iron from ferrihydrite (Fig. 3c). Overall, the experimental results for the mutant demonstrate that the high-affinity siderophores (pyochelin and pyoverdine) of *P. aeruginosa* are not required for efficient acquisition of iron from ferritin.

Role of proteases in acquisition of iron from ferritin

P. aeruginosa is known to secrete several potent proteases that might be involved in acquisition of iron from ferritin through effects on the protein coat. Two experiments addressed the potential role of proteases: (1) growth of *P. aeruginosa* wild-type and

siderophore-free strains in 5 μM iron from 1,500Fe ferritin or uncoated 6L ferrihydrite, in the presence of protease inhibitors (PIC); and (2) a petri-plate-based protease activity assay using cultures grown for 18 h under these conditions. Interference of the PIC/EDTA with the Miller assay precluded analysis of changes in promoter activity.

When ferritin was the iron source, growth of the siderophore-free strain was completely abolished in the presence of the PIC (Fig. 4a), but growth was decreased only moderately for the wild-type strain (Fig. 4c). On plates, casein proteolysis was much more extensive for the siderophore-free strain than for the wild-type strain (Fig. 4d), indicating that the siderophore-free strain secretes more protease, presumably in response to iron deprivation. These observations suggest that siderophores are capable of acquiring iron from the ferritin core without the need for proteases to open a pathway through the protein coat. They further suggest that proteases are important for acquisition of iron from ferritin by non-siderophore-related means.

EDTA, which is a component of the PIC, is a strong iron chelator that could potentially directly increase dissolution rates of the ferrihydrite-structured ferritin core. Growth of the wild-type strain on ferritin was unaffected or at most slightly enhanced in the presence of EDTA alone (Fig. 4c). Growth of the siderophore-free mutant on ferritin was decreased in the presence of EDTA alone (Fig. 4a), but not to the extent observed in the presence of the full PIC. To further test whether EDTA might be enhancing dissolution of the ferrihydrite-structured ferritin core, growth in the presence of ferrihydrite was monitored with the addition of EDTA at a concentration equivalent to that in the PIC. The presence of EDTA did not affect growth of the mutant on ferrihydrite (Fig. 4b). This confirmed that although EDTA likely affects the integrity of ferritin in the presence of *P. aeruginosa*, it does not directly dissolve ferrihydrite to the extent needed to substantially increase growth.

Examination of other possible siderophore-independent pathways

Three types of measurements were made to examine whether other small molecules secreted by *P. aeruginosa* could assist in the solubilization and delivery of iron to the cell: (1) measurement of dissolved iron concentrations in culture supernatants following growth on ferritin; (2) measurement of the iron-reducing capability of the supernatant and cells following culturing of the siderophore-free mutant; and (3) measurement of total pyocyanin concentration in the supernatant follwing culturing of the siderophore-free mutant.

Dissolved iron was measured via ICP-OES in the smaller than 10 kDa fraction of the siderophore-free culture supernatant following growth on 1,500Fe ferritin for 24 h. There was no detectable dissolved iron (i.e., less than 10 μg/l) in this fraction (Table 2), indicating no buildup of a small molecule–iron complex (such as a siderophore–iron complex) in the medium surrounding the cells.

Reduction of Fe(III) to Fe(II) renders iron much more soluble, and eliminates the need for a chelating ligand for iron transit across the outer membrane. We therefore examined the iron-reducing capability of the siderophore-free bacterial cultures. Supernatant aliquots were taken from cultures grown with 1,500Fe ferritin or no added iron at 24 h (late-log phase for the 1,500Fe ferritin cultures, to avoid contamination from dead cells). The aliquots were subjected to the ferrozine assay for Fe(II) as is or sedimented so that the sterile-filtered supernatant could also be assayed (see “Materials and methods”). The measured Fe(III)-reducing activity was strongest in the cell-containing samples, although the supernatant alone was observed to have substantial iron-reducing activity, indicating the likely presence of a secreted reductant (Table 2). *P. aeruginosa* is known to produce and secrete large amounts of redox-active phenazine compounds, such as the blue-green pyocyanin, which are

important for virulence and are overproduced under iron stress [43]. The supernatants for the ferritin-grown cultures bearing reducing activities had a noticeably blue-green color.

Pyocyanin and its precursor phenazine-1-carboxylic acid have both been shown to be capable of Fe(III) reduction [20, 44]. Apparent pyocyanin concentrations were measured via the characteristic UV/vis absorbance λ_{max} of the molecule in the supernatant of the mutant cultures (Table 2). Although this assay is not definitive, if the absorbance were indeed due to pyocyanin, its concentration exceeded the amount of iron reduced in the ferrozine assay (twofold higher under both conditions). This suggests that this compound could be contributing to iron reduction and acquisition by the siderophore-free mutant and wild-type *P. aeruginosa*.

The results obtained using the siderophore-free mutant illustrate a siderophore-independent mechanism for acquiring iron. There was no accumulation of iron in the supernatant at 24 h, even though the supernatant exhibited iron-reducing ability and contained substantial concentrations of a blue-green compound that is potentially pyocyanin. The siderophore-independent mechanism(s) for acquisition of iron from ferritin appear to depend, at least in part, on proteases.

Discussion

Although siderophores are generally important for iron acquisition in pathogens such as *P. aeruginosa*, they are not required when ferritin is the iron source. Here we have shown facile acquisition of iron from the widely abundant soil mineral ferrihydrite and from the caged ferrihydrite biomineral in ferritin, with no dependence on mineral order (i.e., 2L ferrihydrite vs 6L ferrihydrite, and 500Fe ferritin vs 1,500Fe ferritin). And we have observed that secreted proteases are not needed for iron acquisition when siderophores are present, but make critical contributions to siderophore-independent iron acquisition.

The nearly identical kinetics and final culture densities when ferritin was the iron source (Fig. 3b) in the siderophore-free mutant and wild-type *P. aeruginosa* indicates that iron is released from extracellular ferritin and transported into the cells, completely independently of the high-iron-affinity siderophores. The siderophore-independent pathway of acquisition of iron from ferritin appears to depend on exposing the nanomineral surface to solution by means of proteases. Given that Fe(II) is transported readily through the bacterial cell wall, a reducing mechanism is likely. *P. aeruginosa* is known to secrete several reductants, including the blue-green pyocyanin and its metabolic precursor phenazine [19], and their production has been associated with iron deprivation [44, 45]. Iron-reducing activity increased with the extent of iron deprivation and, although not conclusively characterized, could be due to pyocyanin. Notably, pyocyanin and its precursor phenazine-1-carboxylic acid have been shown to reduce iron from ferrihydrite with kinetics sufficient to support *P. aeruginosa* biofilm growth [44]. The Fe(II)-specific permease FeoB was likewise shown to be necessary for transporting the reduced iron across the outer membrane [44]; this is most likely the case in the present study as well, although dependence on FeoB was not directly tested here. The observed lag in the growth curve and lower final culture densities for the siderophore-free mutant relative to the wild type could indicate that the reductant takes longer than siderophores to accrue and become effective in iron acquisition [46].

What role does the ferritin protein cage play in acquisition of iron by *P. aeruginosa?* Ferrihydrite aggregation, observed previously for freeze-dried, free-ferrihydrite samples, which decreases the surface-to-volume ratio, is inhibited by the protein cage. In this sense, the ferritin protein affords “site isolation” for the enclosed iron. However, unless proteases are also present, the protein cage diminishes the availability of iron as indicated by the

critical role of proteases for acquisition of iron from ferritin by the lung pathogen *Burkholderia cenocepacia* [47] and here by the increase in protease activity. Consistent with such results is the ferritin-specific effects of a PIC on attenuation of growth of *P. aeruginosa* on ferritins, contrasting with the protease resistance of growth on ferrihy-drites. This strongly suggests a role for proteases in acquisition of iron from ferritin through protease interactions with the protein coating. Likewise, a recent study of the intracellular pathogen *Burkholderia pseudomallei* demonstrated the robust growth of a siderophore-deficient strain when ferritin was provided as the iron source; although the role of proteases was not tested, this was suggested as a possible mechanism [48].

Ferritin protein cages are relatively stable to the action of general proteases, suggesting that bacteria have specific proteases. Notably, two of the four known proteases secreted by *P. aeruginosa* during infection are regulated by iron and upregulated during iron deficiency [49, 50]. One of these, alkaline protease, is a metalloprotease (AprA); the other, protease IV (PrpL), is a serine protease that has been shown to cleave mammalian transferrin and lactoferrin [49, 51]. PrpL synthesis is regulated via the alternate sigma factor PvdS, which, interestingly, is activated by the pyoverdine/receptor complex during iron deficiency [50]. Although protease inhibitors moderately impair growth of the siderophore-producing wild type on ferritins, the effect is greatly enhanced in the siderophore-free mutant, where growth is completely abolished. We propose that the virulence-associated AprA functions in the uninhibited siderophore-free cultures, because PrpL is produced specifically in response to the presence of pyoverdine. Whether or not other proteases such as elastase may have an effect on ferritin integrity is a question for the future.

Broader implications

Both clinical and environmental bioinorganic chemistry/metallomics will be affected by the new results reported in this study. Clinically, the abnormally high ferritin concentrations in the fluids bathing the lungs of CF patients [11], possibly from cell damage and lysis, could be a growth-promoting source of iron for *P. aeruginosa*, based on the results in this study. The siderophore-independent iron acquisition pathways observed here provide an explanation for the existence of siderophore-free *P. aeruginosa* strains isolated in CF clinical isolates [21, 22] and how siderophore-free bacteria are able to grow and survive in the presence of siderophore-producing strains: the siderophore-free bacterial strains may be competitive at acquiring ferritin iron via a reductive mechanism. Environmentally, bacteria in low-O_2 regions of biofilms should also thrive under the ferritin-rich conditions for the same reasons. These results suggest that strategies for overcoming infections in CF patients need to take into account the full variety of mechanisms, including those pertaining to extracellular ferritin, by which iron can be acquired from human hosts. Similarly, efforts to control microbial bio-films in the environment need to reflect the multiple mechanisms by which bacteria can acquire iron in this setting, including plant ferritin from senescent leaves and seeds. Iron oxyhydroxide nanoparticles, including ferrihydrite and plant- and bacteria-derived ferritins, are broadly abundant in the environment. Most work on aerobic bacteria has focused on the role of siderophores in iron acquisition, but the efficiency of siderophores may be limited by processes such as advection, diffusion, and sorption to clays. These data as well as our previous data on the congener bacterium *Pseudomonas mendocina* [29, 36], which relied on the use of siderophore-free mutants to explore siderophore-related and siderophore-independent iron acquisition mechanisms need to be complemented by more investigation of the complementary exogenous reductants and direct cell–mineral contact [29]. The emerging picture of aerobic microbial iron acquisition is a suite of iron acquisition pathways that must now include, in addition to exogenous organic ligands and reductants [36], the selective behavior, beyond the genus, of microbial species and local mineralogy.

Acknowledgments

Cliff Johnston (Purdue University) performed X-ray diffraction analysis of the ferrihydrite samples. Keshia Koehn and Ewa Dzik (University of Notre Dame) assisted with laboratory experiments. C.D. was partially supported by a Bayer Pre-doctoral Fellowship administered by the Center for Environmental Science & Technology (CEST) at the University of Notre Dame, which also provided use of the ICP-OES and Brunauer–Emmett–Teller adsorption isotherm instruments. Jennifer Szymanowski and William Archer provided assistance with ICP-OES and TEM imaging, respectively; the latter was performed at the Notre Dame Integrated Imaging Facility. Garrett Moraski is thanked for helpful discussions.

References

1. Frederick RE, Mayfield JA, DuBois JL. Biometals. 2009; 22:583–593. [PubMed: 19350396]
2. Nairz M, Schroll A, Sonnweber T, Weiss G. Cell Micro-biol. 2010; 12:1691–1702.
3. Otto BR, Verweijvanvught AMJ, Maclaren DM. Crit Rev Microbiol. 1992; 18:217–233. [PubMed: 1532495]
4. Vasil ML, Ochsner UA. Mol Microbiol. 1999; 34:399–413. [PubMed: 10564483]
5. Wilks A, Burkhard KA. Nat Prod Rep. 2007; 24:511–522. [PubMed: 17534527]
6. Wooldridge KG, Williams PH. FEMS Microbiol Rev. 1993; 12:325–348. [PubMed: 8268005]
7. San Martin CD, Garri C, Pizarro F, Walter T, Theil EC, Nunez MT. J Nutr. 2008; 138:659–666. [PubMed: 18356317]
8. Kumar, V.; Hagler, HK. Interactive case study companion to Robbins pathologic basis of disease, sixth edition (CD-ROM for Windows & Macintosh, individual). Saunders: Philadelphia; 1999.
9. Macedo MF, Cruz E, Lacerda R, Porto G, de Sousa M. Blood Cells Mol Dis. 2005; 35:319–325. [PubMed: 16140024]
10. Reid DW, Lam QT, Schneider H, Walters EH. Eur Respir J. 2004; 24:286–291. [PubMed: 15332399]
11. Stites SW, Plautz MW, Bailey K, O'Brien-Ladner AR, Wesselius LJ. Am J Resp Crit Care Med. 1999; 160:796–801. [PubMed: 10471599]
12. Reid DW, Carroll V, O-May C, Champion A, Kirov SM. Eur Respir J. 2007; 30(2):286–292. [PubMed: 17504792]
13. Reid DW, Anderson GJ, Lamont IL. Am J Phys Lung Cell Mol Phys. 2009; 297:L795–L802.
14. Stites SW, Walters B, O-Brien-Ladner AR, Bailey K, Wesselius LJ. Chest. 1998; 114:814–819. [PubMed: 9743172]
15. Cornell, RM.; Schwertmann, U. The iron oxides: structure, properties, reactions, occurrences, and uses. 2nd edn. Wiley-VCH: Weinheim; 2003.
16. Gilbert B, Ono RK, Ching KA, Kim CS. J Colloid Interface Sci. 2009; 339:285–295. [PubMed: 19709669]
17. Hochella MF Jr, Lower SK, Maurice PA, Penn RL, Sahai N, Sparks DL, Twining BS. Geochim Cosmochim Acta. 2008; 72:A382–A383.
18. Tidmarsin GF, Klebba PE, Rosenberg LT. J Inorg Bio-chem. 1983; 18:161–168.
19. Ingram JM, Blackwood AC. Adv Appl Microbiol. 1970; 13:267–282.
20. Cox CD. Infect Immun. 1986; 52(1):263–270. [PubMed: 2937736]
21. Huston WM, Potter AJ, Jennings MP, Rello J, Hauser AR, McEwan AG. J Clin Microbiol. 2004; 42:2806–2809. [PubMed: 15184477]
22. Martin LW, Reid DW, Sharples KJ, Lamont IL. Biometals. 2011; 24(6):1059–1067. [PubMed: 21643731]
23. Andrews SC. Biochim Biophys Acta Gen Subj. 2010; 1800:691–705.
24. Theil EC. Curr Opion Chem Biol. 2011; 15(2):304–311.
25. Michel FM, Ehm L, Antao SM, Lee PL, Chupas PJ, Liu G, Strongin DR, Schoonen MA, Phillips BL, Parise JB. Science. 2007; 316:1726–1729. [PubMed: 17525301]
26. Michel FM, Barron V, Torrent J, Morales MP, Serna CJ, Boily J, Liu Q, Ambrosini A, Cismasu AC, Brown GE Jr. Proc Natl Acad Sci USA. 2010; 107:2787–2792. [PubMed: 20133643]

27. Liu G, Debnath S, Paul KW, Han W, Hausner DB, Hosein H, Michel FM, Parise JB, Sparks DL, Strongin DR. Langmuir. 2006; 22:9313–9321. [PubMed: 17042547]
28. Michel FM, Hosein H, Hausner DB, Debnath S, Parise JB, Strongin DR. Biochim Biophys Acta Gen Subj. 2010; 1800:871–885.
29. Dehner CA, Barton L, Maurice PA, Dubois JL. Environ Sci Technol. 2011; 45:977–983. [PubMed: 21174456]
30. Hersman LE, Huang A, Maurice PA, Forsythe JH. Geomicrobiol J. 2000; 17(4):261–273.
31. Salas EC, Berelson WM, Hammond DE, Kampf AR, Nealson KH. Geochim Cosmochim Acta. 2010; 74:574–583. [PubMed: 20161499]
32. Barton LE, Grant KE, Kosel T, Quicksall AN, Maurice PA. Environ Sci Technol. 2011; 45(8): 3231–3237. [PubMed: 21294541]
33. Liu XS, Patterson LD, Miller MJ, Theil EC. J Biol Chem. 2007; 282(44):31821–31825. [PubMed: 17785467]
34. Poschet J, Perkett E, Deretic V. Trends Mol Med. 2002; 8:512–519. [PubMed: 12421684]
35. Treffry A, Hawkins C, Williams JM, Guest GR, Harrison PM. J Biol Inorg Chem. 1996; 1:49–60.
36. Dehner CA, Awaya JD, Maurice PA, DuBois JL. Appl Environ Microbiol. 2010; 76(7):2041–2048. [PubMed: 20118367]
37. Schwertmann, U.; Cornell, RM. Iron oxide in the laboratory: preparation and characterization. Weinheim: Wiley-VCH; 2000.
38. Choi KH, Gaynor JB, White KG, Lopez C, Bosio CM, Karkhoff-Schweizer RR, Schweizer HP. Nat Methods. 2005; 2(6):443–448. [PubMed: 15908923]
39. Miller FD, Hershberger CL. Gene. 1984; 29:247–250. [PubMed: 6092227]
40. Stookey LL. Anal Chem. 1970; 42:779.
41. Essar DW, Eberly L, Hadero A, Crawford IP. J Bacteriol. 1990; 172:884–900. [PubMed: 2153661]
42. Kurachi M. Bull Inst Chem Res Kyoto Univ. 1958; 36:174–187.
43. Lau GW, Ran H, Kong F, Hassett DJ, Mavrodi D. Infect Immun. 2004; 72(7):4275–4278. [PubMed: 15213173]
44. Wang Y, Wilks JC, Danhorn T, Ramos I, Croal L, Newman DK. J Bacteriol. 2011; 193(14):3606–3617. [PubMed: 21602354]
45. Newman DK. Nat Chem Biol. 2006; 2:71–78. [PubMed: 16421586]
46. Dhungana S, Crumbliss AL. Geomicrobiol J. 2005; 22:87–98.
47. Whitby PW, Van Wagoner TM, Springer JM, Morton DJ, Seale TW, Stull TL. J Med Microbiol. 2006; 55:661–668. [PubMed: 16687582]
48. Kvitko BH, Goodyear A, Propst AL, Dow SW, Schweizer HR. PLoS Negl Trop Dis. 2012; 6(6):e1715. [PubMed: 22745846]
49. Shigematsu T, Fukushima J, Oyama M, Tsuda M, Kawamoto S, Okuda K. Microbiol Immunol. 2001; 45:579–590. [PubMed: 11592632]
50. Wilderman PJ, Vasil AI, Johnson Z, Wilson MJ, Cunliffe HE, Lamont IL, Vasil ML. Infect Immun. 2001; 69:5385–5394. [PubMed: 11500408]
51. Vartivarian SE, Cowart RE. Arch Biochem Biophys. 1999; 364:75–82. [PubMed: 10087167]

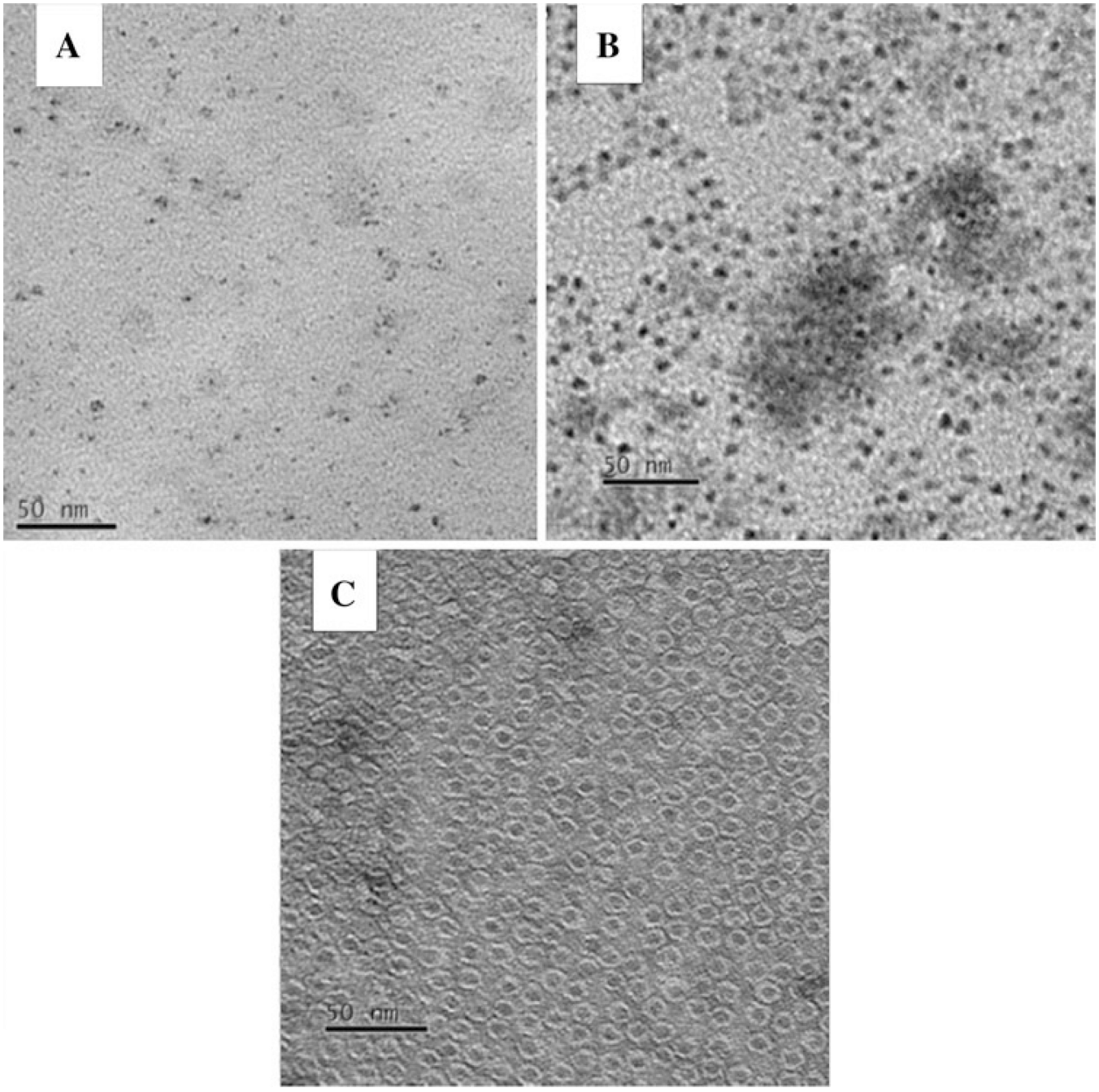

Fig. 1.

Integrity of the ferrihydrite mineral cores of iron-loaded ferritin samples. Transmission electron microscopy images show the iron-containing cores of **a** low-iron-loaded ferritin (500Fe ferritin) and **b** high-iron-loaded ferritin (1,500Fe ferritin). **c** The 1,500Fe ferritin stained with uranyl acetate shows the ferritin protein cage surrounding the core. *Scale bars* represent 50 nm in length

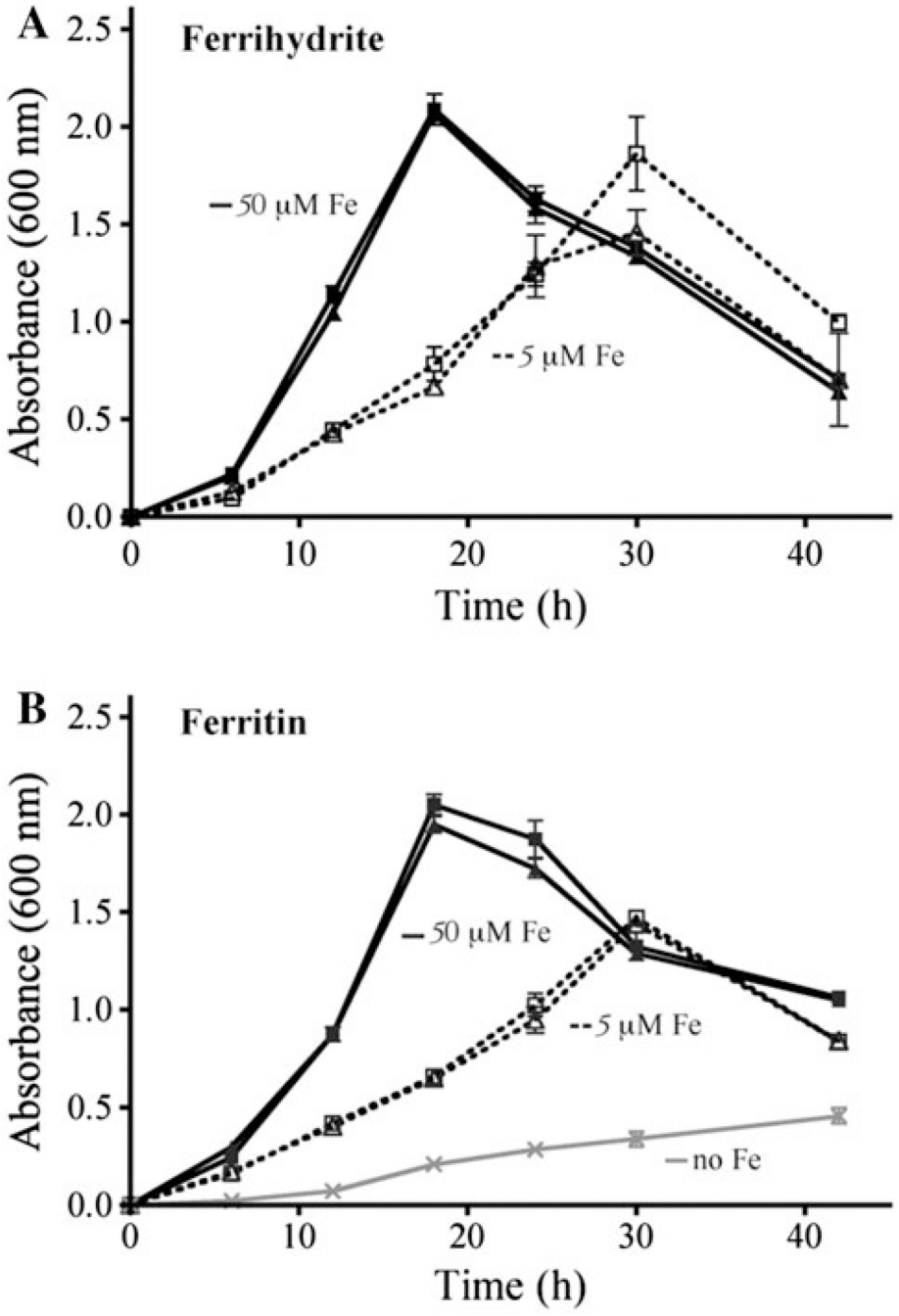

Fig. 2.

Two-line (2L) and four-line (4L) ferrihydrites and their protein-coated ferritin counterparts act as equivalent iron sources for *Pseudomonas aeruginosa*. Comparison of **a** ferrihydrite and **b** ferritin as iron sources for wild-type *P. aeruginosa*. The iron sources were initially present at a concentration of either 50 or 5 μM iron. *Triangles* represent 6L ferrihydrite or 1,500Fe ferritin, which encloses a structurally similar nanoparticle. *Squares represent* 2L ferrihydrite or 500Fe ferritin. A control with no added iron is shown for comparison in **b**

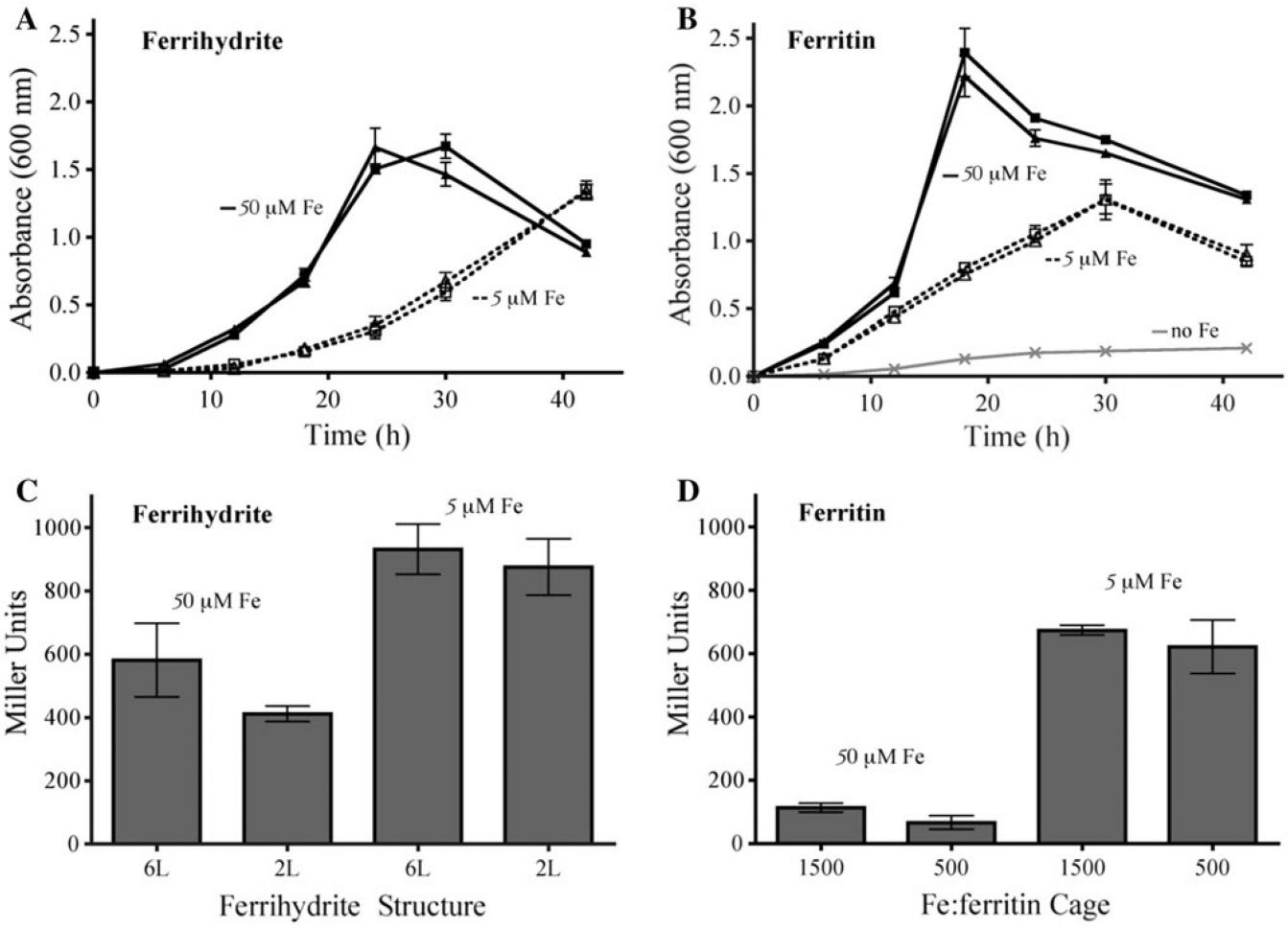

Fig. 3.

The presence or absence of siderophores does not affect growth kinetics and has little effect on sensed iron deficiencies in *P. aeruginosa* grown on ferrihydrites or ferritins. Comparison of **a** ferrihydrite and **b** ferritin as iron sources for siderophore-free (Δ*pvdD*Δ*pchEF*) *P. aeruginosa*. The iron sources were initially present at a concentration of either 50 or 5 μM iron. *Triangles* represent 6L ferrihydrite or 1,500Fe ferritin, which encloses a structurally similar nanoparticle. *Squares* represent 2L ferrihydrite or 500Fe ferritin. A control with no added iron is shown for comparison in **b**. P_{pvdA} promoter activity from the cultures in a and b, reporting on the level of iron starvation in the cells after 18 h of growth, is plotted in **c** and **d**, respectively

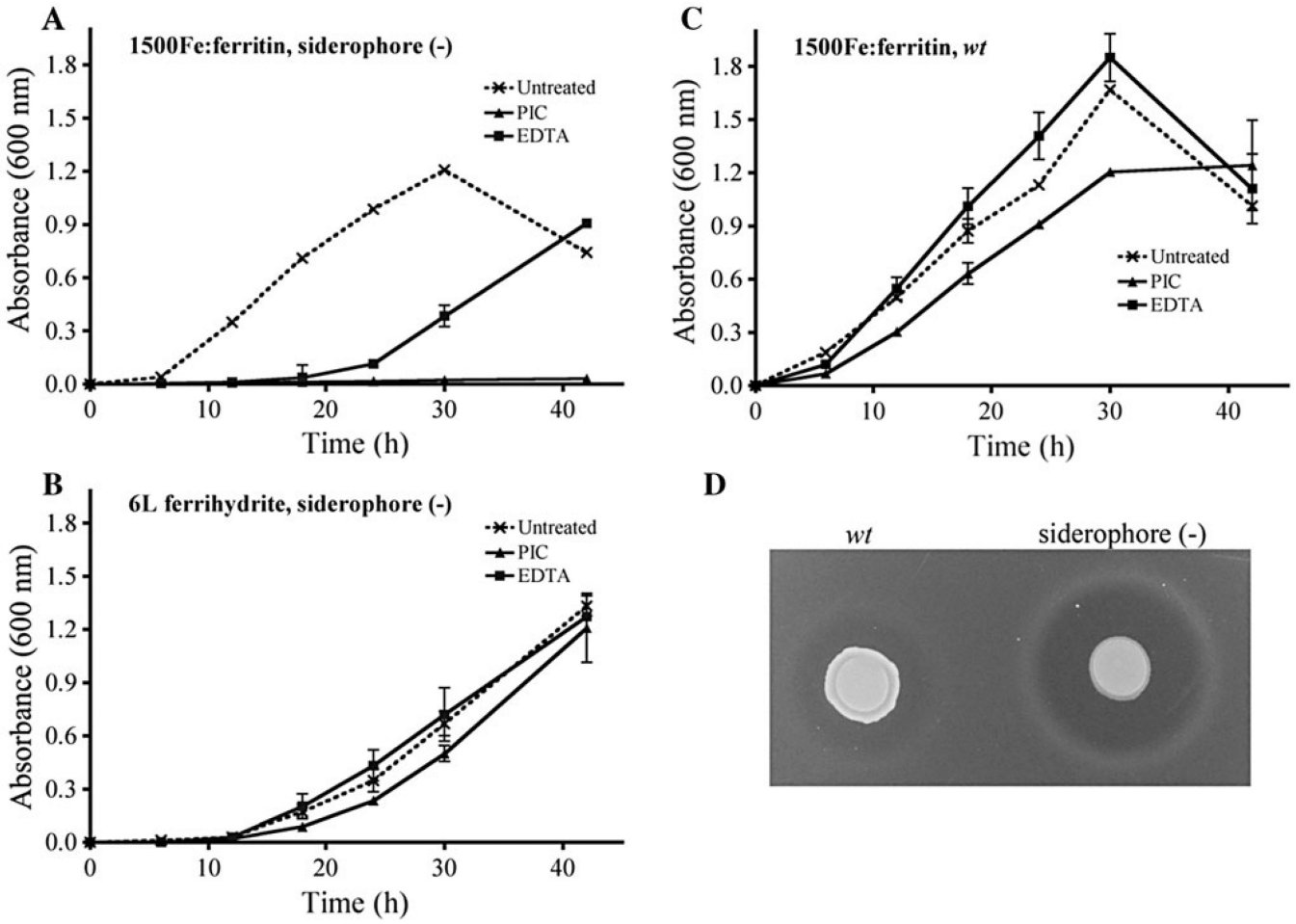

Fig. 4.

In the absence of siderophores, growth of *P. aeruginosa* on ferritins depends on proteases. Siderophore-free cultures were grown on 5 μM iron from **a** 1,500Fe ferritin or **b** 6L ferrihydrite, and supplemented with a protease inhibitor cocktail (PIC) or EDTA (a component of the **PIC**), as indicated. Growth of wild-type *P. aeruginosa* on 1,500Fe ferritin is illustrated in **c**. Proteolytic activity from cultures grown on 1,500Fe ferritin for 18 h is illustrated in **d**. A wide zone of casein depletion is observed for the siderophore-free mutant relative to the wild type. This indicates that the mutant strain grown on ferritin has stimulated protease activity relative to the wild type. *wt* wild type

Table 1

Bacterial strains, plasmids, and primers used in this study

Strains, plasmids, or primers	Description	References
Strains		
Pseudomonas aeruginosa PAO1[a]	Wild-type strain	[23]
PAO1 Δ*pvdD*Δ*pchEF*	Siderophore (pyoverdine and pyochelin) mutant strain	[3]
P. aeruginosa PAO1::P_{pvdA}-*lacZ*	Mini-Tn7T-P_{pvdA}-lacZ-Gm integrated into *P. aeruginosa* wild-type strain	This study, [10]
PAO1 Δ*pvdD*Δ*pchEF*::P_{pvdA}-*lacZ*	Mini-Tn7T-P_{pvdA}-lacZ-Gm integrated into *P. aeruginosa* siderophore mutant strain	This study, [10]
Plasmids		
pUC18-mini-Tn7T-*lacZ*-Gm	Plasmid backbone for promoter-*lacZ* fusion strains	[6]
pTNS2	Helper plasmid for pUC18	[6]

[a] *P. aeruginosa* PAO1 wild-type strain was obtained from Joshua Shrout of the Department of Civil and Environmental Engineering and Earth Sciences, University of Notre Dame

Table 2

Iron reduction activity of siderophore-free (Δ*pvdD*Δ*pchEF*) *P. aeruginosa* cultures after 24 h growth

Iron source	Iron reduction activity [μmol Fe(II) cell/min × 10^{-10}][a,b]	Total iron reduced in supernatant (μM)[a]	Total pyocyanin in supernatant (μM)
No iron	3.9 (0.2) (whole cells)	2.92 (0.08)	5.90 (0.01)
	2.8 (0.08) (supernatant)		
1,500Fe ferritin[c]	3.0 (0.2) (whole cells)	6.18 (0.65)	14.28 (0.76)
	0.98 (0.1) (supernatant)		

For all measurements, average values for three replicates are reported with standard deviations in *parentheses*

[a] Ferrozine assay measures the absorbance of the Fe(II)–ferrozine complex at 562 nm

[b] The concentration of solubilized iron in the culture supernatants was below the detection limit of inductively coupled plasma optical emission spectroscopy (below 10 μg/l)

[c] Ferritin was added to a final concentration of 5 μM iron